



# Contactless Condition Monitoring of 11kv Glass Insulators using Image Fusion by cGAN Technique

Priya Sankar Mandal<sup>1</sup>, Sudipta Mondal<sup>2</sup>, Shirsendu Chakraborty<sup>3</sup>, Rajat Kumar Mandal<sup>4</sup>,  
Birendra Krishna Ghosh<sup>5</sup>, Mitul Ranjan Chakraborty<sup>6</sup>, Milan Basu<sup>7</sup>

<sup>1,2,3</sup> Students, and <sup>4,5,6,7</sup> Faculty  
Department of Electrical Engineering,  
Techno International New Town,  
Kolkata, India.  
[birendraee@gmail.com](mailto:birendraee@gmail.com)

**Abstract:** Insulators play a crucial role in safeguarding electrical power systems, but their effectiveness can be compromised by aging and surface contamination caused by pollutants. Monitoring the condition of insulators is essential to replace them before reaching the end of their functional life. While traditional methods like monitoring electrical surface discharge (ESDD) values or leakage current provide reliable results, implementing them in continuous monitoring systems can be challenging. Contactless monitoring methods, such as infrared thermography, have gained attention for accurately predicting insulator contamination levels. Enhancing accuracy is possible by combining visible and infrared features, yet infrared cameras are costly and complex to operate. Visible range image-based monitoring, on the other hand, yields subpar results without extensive data processing. This paper introduces a novel contactless condition monitoring technique using only visible range images of insulators. A conditional Generative Adversarial Network (cGAN) algorithm is employed to synthetically generate infrared images from visible range images. The resulting infrared image is fused with the original visible range image, and the combined image is input into a Convolution Neural Network (CNN) architecture trained for visible-infrared fusion image feature extraction. The novelty of this approach described contactless condition monitoring with favorable accuracy and offer a safe cost-effective alternative to traditional methods.

**Keywords:** Condition Monitoring, Contamination, cGAN, IR Images

## 1. INTRODUCTION:

Power systems commonly involve high voltage applications and utilize costly machinery operated by human personnel. Insulators made of non-conductive materials like ceramic, porcelain, glass, and polymers, act as protective devices for both equipment and human safety within the system. Maintaining insulators in optimal condition is crucial due to their vital protective functions. Apart from natural aging, insulators face the risk of accumulating contaminants and pollutants on their surfaces. Moisture exposure can lead to the formation of a conductive contaminant layer, causing non-uniform leakage current and the development of dry bands on the insulator's external housing. This process intensifies leakage current flow and may result in flashovers, rapidly degrading the insulator's condition and impeding its protective capabilities. As many insulators are situated outdoors, ongoing and thorough monitoring for surface contamination is essential. The extent of deterioration varies among insulator materials, with polymer insulators like silicon rubber being more resistant due to their hydrophobic nature. However, polymer insulators are not entirely immune to contaminant accumulation effects, and their hydrophobicity diminishes with age. Thus, condition monitoring remains critical for silicon rubber insulators, similar to insulators of other materials.

Various measures and methods assess the extent of contamination in an insulator. Traditional measures include Equivalent Salt Deposit Density (ESDD) and Non-Soluble Deposit Density (NSDD), which are accurate but cumbersome and time-consuming. Leakage current analysis, directly related to ESDD, is a popular method but challenging to implement continuously. Infrared thermography, a non-contact technique, enables continuous and non-intrusive contamination level detection by analyzing infrared images. However, it requires expensive and complex infrared cameras.

This paper introduces a condition monitoring method using only visible range images. A conditional



Generative Adversarial Network (cGAN) generates thermal images from visible range images. The generated thermal image is fused with the original visible range image using an unsupervised feature extraction algorithm called latent low rank representation (LatLRR). The resulting visible-infrared (VIS-IR) fusion image is fed into a pre-trained ResNet50, CNN architecture for effective feature extraction and accurate classification of the insulator's contamination level.

## 2. EXPERIMENTAL SETUP:

A polymeric-encased MOSA sample running at 11kV was selected for the testing stage. This letter focuses on evaluating surface contamination on the MOSA sample using the solid layer method. It is important to emphasize that the SLM surface contamination experiment followed IEC60507 rules to the letter. Fig 1 shows the experimental setup for capturing the raw IR image for insulators. Hv transformer is used to supply power to insulator through a control unit and water resistance. With the help of High resolution IR camera image has been captured step by step by increasing supply voltage up to break down voltage. Fig 1 shows practical setup by which IR image and visual image has been captured. Physical parameters like operating voltage, creepage distance are tabulated in Table 1. Experiment performed based on single disc at a time.

Fig. 1. Experimental setup

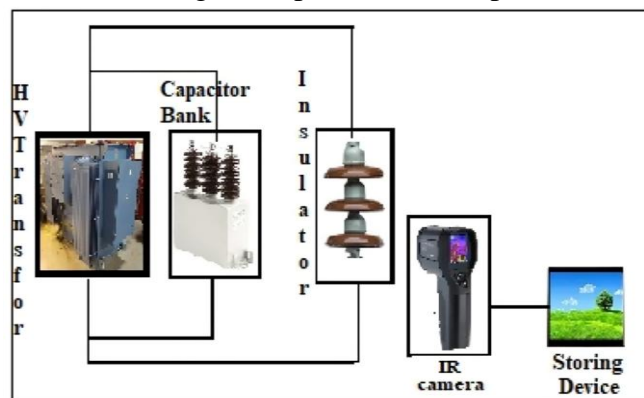


Table 1- Parameters of Overhead line Insulator

Sl. No.	Parameter	Value
1	Nominal Voltage	11 KV
2	Creepage Distance	255mm
3	Pin Diameter	20mm
4	Height	145mm
5	No of Disc	1

## 3. PIX2PIX GAN BASED IMAGE-TO-IMAGE TRANSLATION:

To achieve the target of using just visible (VIS) photos, we solve the lack of infrared thermal (IRT) images by creating synthetic IRT images from the VIS images. This is performed via a technique known as image-to-image translation, which we execute effectively using generative adversarial networks (GANs). Fig 3 shows the architecture of PIX2PIX GAN technology. Generative adversarial networks (GANs) represent a framework aimed at approximating generative models, employing an adversarial process involving two concurrently trained models: the generator and the discriminator. Pix2Pix emerges as a notably successful deep learning model designed for paired image translation, leveraging a conditional GAN structure. The generator's task is to generate plausible data, while the discriminator is trained to differentiate between artificially generated and authentic data. Similar to traditional GAN setups, Pix2Pix incorporates both a generator and a discriminator. Initially, grayscale input images are inputted into the generator, which subsequently produces corresponding colorized versions. In the



Pix2Pix architecture, the generator typically employs a convolution network utilizing a U-net or encoder-decoder design. In this work, features have been extracted from photos using a Pix2Pix GAN. Fig 4 shows the output of Pix2Pix GAN. Left most image shows real capture image and right most image represents Pix2Pix generated fused image.

Fig. 2. Architecture of Pix2Pix GAN technology

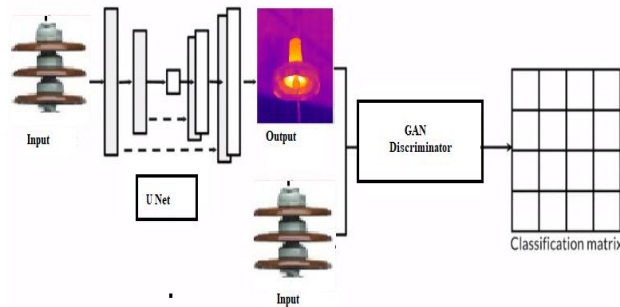
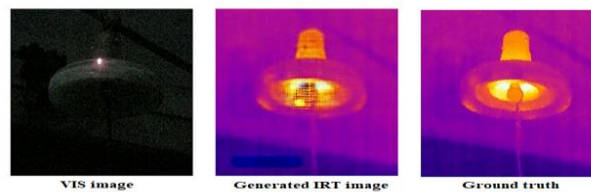


Fig. 3. Fused image using Pix2Pix GAN technology



#### 4. LATLRR BASED VIS-IR IMAGE FUSION:

After data augmentation image has been converted into grayscale image using LatLRR based VIS-IR image fusion technique. Fig 2 shows the practically capture IR image and converted grayscale image. Traditional transform-based fusion methods, such as the discrete wavelet transform (DWT), are widely employed but often fall short in preserving intricate details. On the other hand, Convolution Neural Network (CNN) based image fusion encounters challenges with small-sized datasets. To overcome these limitations, we leverage the latent low-rank representation (LatLRR) technique for image fusion.

Latent Low-Rank Representation (LatLRR) is a technique used in machine learning and computer vision for data representation and dimensionality reduction. It decomposes a data matrix into two low-rank matrices, a representation matrix and a latent matrix, to represent high-dimensional data in a lower-dimensional latent space. LatLRR uses low-rank decomposition techniques to factorize the data matrix into a product of two low-rank matrices, capturing the underlying structure or patterns. LatLRR also introduces latent variables, which capture hidden or unobserved factors influencing data distribution. These variables are then optimized using techniques like gradient descent to minimize the loss function. LatLRR is applied to tasks like dimensionality reduction, data denoising, feature extraction, clustering, and image classification in computer vision. It combines the benefits of low-rank decomposition with latent variable models, improving performance in machine learning tasks, especially when dealing with complex and structured data. As per Fig 4 LatLRR approach involves decomposing base feature image and saliency feature image into their low-rank and saliency components. The low-rank features are amalgamated using a weighted mean strategy, aiming to capture essential information efficiently. Meanwhile, the saliency features undergo fusion using a sum strategy, emphasizing distinctive and significant details. The final fusion image is then crafted by combining the base part, encompassing the low-rank representation, and the salient detail part, ensuring a comprehensive and detailed representation in the fused result.

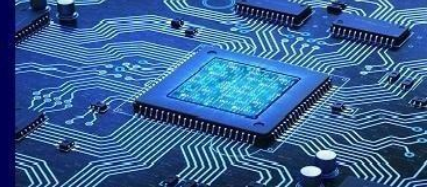


Fig. 4. IR image to converted Grayscale

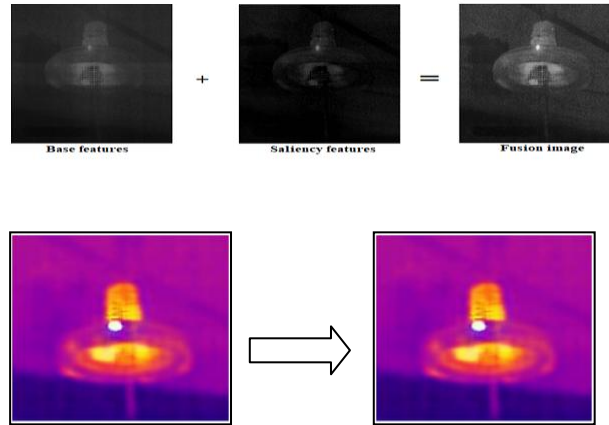
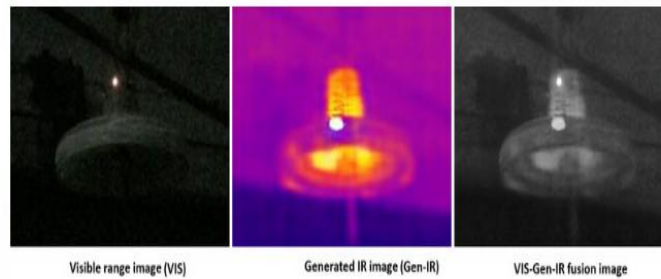


Fig. 5. Fused image using Pix2Pix GAN technology



The flowchart in Figure 6 outlines the suggested methodology, which involves several sequential steps for processing images to achieve specific goals. Initially, an RGB image is captured and stored externally before being resized to a standard resolution of 640x480 pixels. Then, using the PIX2PIX GAN technique, the image is divided into two segments, each measuring 217x217 pixels. Concurrently, an Infrared (IR) image is generated and resized to match the dimensions of the RGB image. The next phase involves merging the RGB and IR images using the Latent Low-Rank Representation (LatLRR) method to create a composite image that combines the strengths of both modalities. Finally, the fused image undergoes classification using Convolutional Neural Network (CNN) algorithms for automated analysis and labeling. Overall, this methodology employs a systematic approach integrating cutting-edge techniques to extract meaningful insights from input imagery for various applications.

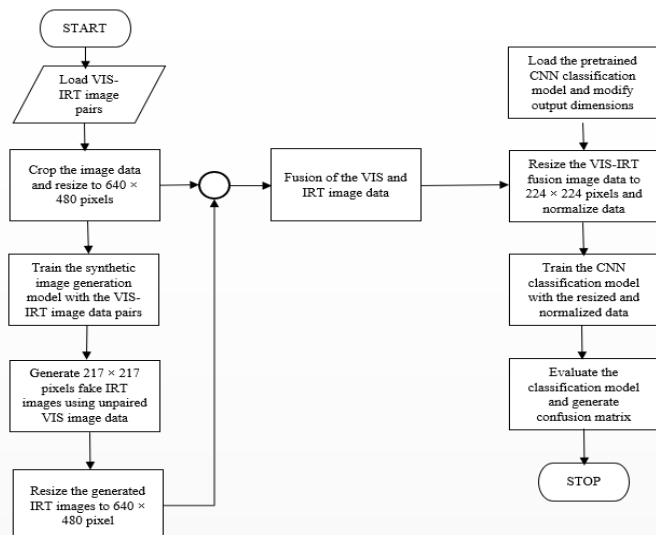




Fig. 6. Flowchart of proposed methodology

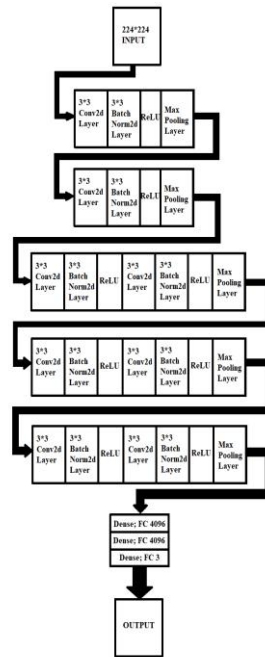
## 5. VGG16 BASED FEATURE EXTRACTION AND CLASSIFICATION:

Deep learning Convolution Neural Network (CNN) classification models exhibit superior performance compared to traditional classification models. Among these, the Visual Geometry Group Network (VGGNet) stands out as the most widely adopted deep learning CNN architecture for image recognition and classification tasks. In our implementation, we utilized the VGG16 architecture, named for its 16 convolution layers.

VGG16 functions by receiving an RGB image of size 224x224 pixels as input. This image progresses through a sequence of 13 convolutional layers, where filters are applied to extract features across various scales. Following each convolutional layer, Rectified Linear Unit (ReLU) activation functions introduce nonlinearities into the network. Max-pooling layers then reduce the spatial dimensions of the feature maps, enhancing abstraction. The resulting features from the convolutional layers are flattened and processed by three fully connected layers, performing sophisticated reasoning based on the extracted features. The final fully connected layer employs a softmax activation function to generate class scores, indicating the probabilities of the input image belonging to different classes. Throughout the training process, the parameters of both convolutional and fully connected layers are adjusted via backpropagation and optimization methods like stochastic gradient descent (SGD). VGG16 commonly serves as either a feature extractor or a pretrained model for tasks in computer vision. Utilizing transfer learning, it can be fine-tuned to suit specific datasets, even when training data is limited. To sum up, VGG16 learns hierarchical representations of input images through convolutional and pooling layers, culminating in classification through fully connected layers.

CNN architectures tend to be less effective when trained on a small-sized dataset. To address this challenge, we opted for a VGG16 classification model that had been pre-trained on the ImageNet dataset. This pre-training enhances the model's ability to generalize features and improves its performance, especially when dealing with limited data.

Fig. 7 Architecture of technology VGG16.



## 6. RESULT AND DISCUSSION:

For this classification model, simulation has been conducted with various CNN architectures of similar depth, including VGG11, VGG16, VGG19, and ResNet18. Among these architectures, VGG16 exhibited the highest accuracy, reaching 90.62%. Fig 8 shows a comparative study on VGG11, VGG16, VGG19, and ResNet18.

Fig. 8. Confusion matrix of VGG16

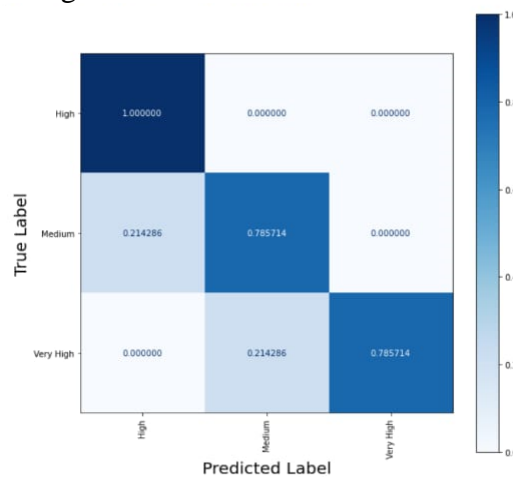


Fig. 9. Scattered plot of VGG16

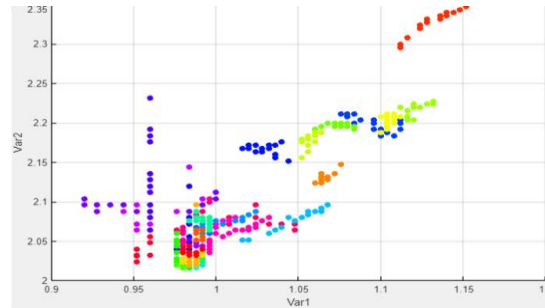


Table 2 - Table Type Styles

Classification Method	Accuracy (%)	Sensitivity (%)	Computation Time(ms)
VGG11	87.5	82.1	1.21
<b>VGG16</b>	<b>90.62</b>	<b>85.6</b>	<b>1.02</b>
VGG19	85.47	84.3	0.96
ResNet18	85.94	83.2	1.06

Furthermore, when applying our ground truth dataset to the same VGG16 classification model, we achieved an even higher accuracy of 90.62%. This outcome underscores the effectiveness of the synthetic IRT images generated within our framework, a conclusion supported by an average structural similarity index measure (SSIM) value of 0.928. Additionally, we validated that the fusion of visible (VIS) and infrared thermal (IRT) images enhances performance. When the classification model was exclusively trained and evaluated using IRT images, the accuracy reached 77.78%. This comparison reinforces the value of integrating both VIS and IRT images for improved classification accuracy.

## 7. CONCLUSION:

The study presents a thorough approach for assessing the level of surface contamination on glass insulator using infrared thermal (IRT) pictures. This framework blends base feature colour characteristics with deep features to achieve successful categorization. The findings show that using the suggested fusion strategy improves classification performance significantly. Notably, the ensemble framework has extremely high precision, making it ideal for real-time surface condition evaluation of glass insulators during operation. This architecture has the intrinsic benefit of allowing for remote monitoring of insulator. Furthermore, its performance is unaffected by changes in the backdrop, resulting in robust and dependable assessments. With knowledge of surface contamination levels, preventive interventions may be performed to prevent undesirable failures in suspension insulators. Increase safety, user friendly and economic method of condition monitoring is the basic novelty of the proposed methodology. It is also observed that classification accuracy is more than 90% and less time consuming. In future a hardware can be constructed to transmit real time data directly to make it more effective in real time.

## 8. REFERENCES:

- [1] L. Wang, B. Cao, H. Mei, C. Zhao, and Z. Guan, "Effects of natural contamination components on the surface conductivity under saturated moisture", IEEE Transactions on Dielectrics and Electrical Insulation, vol. 24, no. 5, pp. 2945-2951, October 2017.
- [2] A. A. Salem, R. Abd-Rahman, S. A. Gailani, M. S. Kamarudin, H. Ahmad, and Z. Salam, "The Leakage Current Components as a Diagnostic Tool to Estimate Contamination Level on High Voltage Insulator", IEEE Access, vol. 8, pp. 92514-92528, May 2020.
- [3] M. Albano, R. T. Waters, P. Charalampidis, H. Griffiths, and A. Haddad, "Infrared analysis of dry-band flashover of silicone rubber insulators", IEEE Transactions on Dielectrics and Electrical Insulation, vol. 23, no. 1, pp. 304-310, February 2016.
- [4] Y. Lin, P. Chiang, and S. Miaou, "Enhancing Deep-Learning Object Detection Performance Based on Fusion of Infrared and Visible Images in Advanced Driver Assistance Systems", IEEE Access, vol. 10, pp. 105214-105231, October 2022.



2022.

- [5] X. Qian, M. Zhang, and F. Zhang, "Sparse GANs for Thermal Infrared Image Generation From Optical Image", *IEEE Access*, vol. 8, pp. 180124-180132, September 2020.
- [6] I. Kimoto, T. Fujimura and K. Naito. "Performance of Insulators for Direct Current Transmission Line Under Polluted Condition", *IEEE Trans. Power App. Syst.*, Vol.92, No. 3, pp. 943-949, 1973.
- [7] C. Zhang, L. Wang and Z. Guan, "Investigation of DC discharge behavior of polluted porcelain post insulator in artificial rain," *IEEE Trans. Dielectr. Electr. Insul.*, vol. 23, no. 1, pp. 331-338, February 2016.
- [8] Y. Taniguchi, N. Arai and Y. Imano, "Natural Contamination test of Insulators at Noto Testing Station Near Japan Sea", *IEEE Trans. Power App. Syst.*, Vol.98, No. 1, pp. 239-245, 1979.
- [9] W. Lampe, T. K. E. Hoglund, C. L. Nellis, P. E. Renner and R. D. Stearns, "Long-term tests of HVDC insulators under natural pollution conditions at the Big Eddy Test Center", *IEEE Trans. Power Del.*, Vol.4, No. 1, pp. 248-259, 1989.
- [10] L. Li, Y. Li, M. Lu, Z. Liu, C. Wang and Z. Lv, "Quantification and comparison of insulator pollution characteristics based on normality of relative contamination values," *IEEE Trans. Dielectr. Electr. Insul.*, Vol.23, No. 2, pp. 965-973, April 2016.
- [11] N. A. Wogman, "Natural Contamination in Radionuclide Detection Systems," in *IEEE Trans. Nuclear Science*, Vol. 28, No. 1, pp. 275-281, 1981.
- [12] K. Takasu, T. Shindo and N. Arai, "Natural contamination test of insulators with DC voltage energization at inland areas", *IEEE Trans. Power Del.*, Vol.3, No. 4, pp. 1847-1853, 1988.
- [13] J. Wang, K. Wang, M. Zhou and L. Zhao, "The natural contamination of XP-70 insulators in Shenzhen, China", *IEEE Trans. Dielectr. Electr. Insul.*, Vol.23, No. 1, pp. 349-358, 2016.
- [14] Y. Taniguchi, N. Arai and Y. Imano, "Natural Contamination test of Insulators at Noto Testing Station Near Japan Sea", *IEEE Trans. Power App. Syst.*, Vol.98, No. 1, pp. 239-245, 1979.
- [15] Z. Zhang, D. Zhang, X. Jiang and X. Liu, "Study on natural contamination performance of typical types of insulators," *IEEE Trans. Dielectr. Electr. Insul.*, Vol. 21, No. 4, pp. 1901-1909, August 2014.
- [16] B. Dong, X. Jiang, Z. Zhang, J. Hu, Q. Hu and L. Shu, "Effect of environment factors on ac flashover performance of 3 units of polluted insulator strings under natural fog condition," *IEEE Trans. Dielectr. Electr. Insul.*, Vol. 21, No. 4, pp. 1926-1932, August 2014.
- [17] Z. Zhang, D. Zhang, X. Jiang, X. Liu, "Study on natural contamination performance of typical types of insulators", *IEEE Trans. Dielectr. Electr. Insul.*, Vol.21, No. 4, pp. 1901-1909, 2014.
- [18] F. Zhang, J. Zhao, L. Wang and Z. Guan, "Experimental Investigation on Outdoor Insulation for DC Transmission Line at High Altitudes," *IEEE Trans. Power Del.*, Vol. 25, No. 1, pp. 351-357, Jan. 2010.
- [19] Selection and dimensioning of high-voltage insulators intended for use in polluted conditions-Part 1: Definitions, information and general principles, IEC/TS 60815-1, 2008.
- [20] J. Wardman, T. Wilson and P. Bodger, "Volcanic ash contamination: limitations of the standard ESDD method for classifying pollution severity," *IEEE Trans. Dielectr. Electr. Insul.*, Vol. 20, No. 2, pp. 414-420, April 2013.